# HYDRATION MECHANISMS OF CALCIUM SULPHOALUMINATE $C_4A_3\bar{S}$, $C_4A\bar{S}$ PHASE AND ACTIVE BELITE β-$C_2S$

H. EL-DIDAMONY, T. M. EL-SOKKARI*, KH. A. KHALIL, #MOHAMED HEIKAL**, I. A. AHMED

*Chemistry Department, Faculty of Science, Zagazig University, Zagazig, Egypt*
**Housing and Building Research Centre, Cairo, Egypt*
*** Chemistry Department, Faculty of Science, Benha University, Benha, Egypt*

#E-mail: ayaheikal@hotmail.com

Submitted March 10, 2012; accepted September 3, 2012

**Keywords:** Calcium sulphoaluminate ($C_4A_3\bar{S}$), β-dicalsium silicate (active belite), Hydration characteristics, XRD and DSC

*Highly reactive belite and calcium sulphoaluminate as well as monosulphate mix were prepared from nano-materials at lower temperatures ~1250°C. The crystal size of these materials was 25, 16 and 27 nm as determined from the X-ray analysis. The sulphoaluminate belite cement is a recent type of cement prepared at lower temperature with good properties. The aim of the present work is to synthesize $C_4A_3\bar{S}$, monosulphate mix $C_4A\bar{S}$ and active belite β-$C_2S$. The hydration mechanism was studied by XRD and DSC techniques as well as by the determination of chemically combined water contents of cement pastes with curing time. The results reveal that ettringite is first formed hydrates in the monosulphate mix, which then converted into monosulphate hydrates. The results of DSC and XRD are in good agreement with those of combined water contents. On the other side, the rate of hydration of active belite increases linearly from 3 up to 90 days, whereas, the traditional belite hydrates increase with lower rate up to 90 days, due to the thermodynamic stability structure of traditional belite.*

## INTRODUCTION

Nano-materials show unique physico-chemical properties can be lead to the development of more effective materials than once which are currently available [1]. It was found that nano-particles uniformly dispersed in a cement paste will accelerate cement hydration due to their activity [1]. Additionally, nano-particles will fill the open pores to increase strength and improve the microstructure of cement and the interface between the cement paste, mortar and aggregates in concrete [2]. Application of nano-materials into the production of cement and concrete can lead to improvements in civil infrastructure because the mechanical strength and life of concrete structures are determined by the microstructure and by the mass transfer in nano-scale [2]. Additional studies have also concluded that nano-$SiO_2$ added to high-volume fly ash strength concrete (HFAC) could improve short and long term strengths [3].

Ginebara et al., [4] reported that particle size can greatly affect the kinetics of cement hydration. It was indicated that a reduction in particle size can lead to a more rapid setting and hardening of cement due to stronger electrostatic attractive forces and a greater specific surface.

In addition, the nano-particles will fill pores and increase the strength which lead to improve the microstructure of cement pastes and the boundary between the cement pastes and aggregates in concrete [1]. The major problem is with β-$C_2S$ cement that reacts very slowly and gives very little strength at the early ages of hydration. Lower reactively of β-$Ca_2SiO_4$ is due to its higher thermodynamic stability and dense packing structure [5, 6]. In order to enhance the hydraulic hardening capacity of belite cements to produce highly reactive β-dicalcium silicate. It has been prepared using nano-materials such as $Ca(NO_3)_2$ and nano-silica at lower temperature up to 1250°C [7].

Calcium sulphoaluminate cements are seen as a very attractive high–performance material. Rapid strength and durability in aggressive environments make it appropriate to civil engineering requests. It achieves self desiccation more readily than OPC compositions and affords protection against corrosion to embedded steel, evening cyclic exposure to seawater. Its high sulfate content tends to increase the resistant to seawater attack, because its constituent phases are fully sulfated [8].

In the present paper highly reactive β-$Ca_2SiO_4$ have been prepared from nano-$SiO_2$, and nano-$Ca(NO_3)_2$. Also, $C_4A_3\bar{S}$ and $C_4A\bar{S}$ are prepared from nano-materials such as nano-$Al(OH)_3$ and nano-$Ca(NO_3)_2$ with pure gypsum. The rate of hydration of β-$C_2S$, $C_4A_3\bar{S}$ and $C_4A\bar{S}$ can be studied by the determination of free lime, insoluble residue contents as well as by the aid of DSC and XRD techniques.

## EXPERIMENTAL

The materials used in this work were nano-Ca $(NO_3)_2$, nano-$Al(OH)_3$, nano-silica and $CaSO_4 \cdot 2H_2O$ from Prolabo Company. The nano-$Al(OH)_3$ was prepared from Al-dross after leaching with HCl then precipitated by ammonia solution at pH = 8 [9]. Nano-silica was also synthesized by acid hydrolysis of sodium silicate $Na_2SiO_3$ using 0.5N HCl and slowly stirred at 60°C at pH between 1 and 2 [10]. $Ca(NO_3)_2$ was freshly prepared by the addition of nitric acid (1:1) to $CaCO_3$ to complete reaction then evaporated at 60°C until solidification. The powder of $Ca(NO_3)$ was dried at 50°C for 24 hours [11].

The calcium sulphoaluminate phase ($C_4A_3\bar{S}$), monosulphate ($C_4A\bar{S}$) and active belite ($\beta$-$C_2S$) were prepared from the stoichiometric amounts of nano-$Ca(NO_3)_2$, nano-$Al(OH)_3$, nano-$SiO_2$ and precipitated $CaSO_4.2H_2O$ [12]. Figures 1, 2 show TEM micrograph of nano-silica and $Al(OH)_3$ with crystal size 13 and 38 nm.

The traditional belite was synthesized from traditional reagent grade $CaCO_3$ and $SiO_2$ quartz in the proper molar ratios by firing the mixture twice at1450°C for one hour using $B_2O_3$ (0.5 %) as stabilizer. The fired belite contains 0.15 % free lime then ground to the surface area 3500 $cm^2/g$ [13]. The chemical analysis of the fired materials is seen in Table 1.

Each mix of calcium sulphoaluminate ($C_4A_3\bar{S}$), monosulphate ($C_4A\bar{S}$) and active belite ($\beta$-$C_2S$) phase was mixed with the suitable amount of water of consistency [14], then pressed in one inch cubic moulds. The moulds were cured in humidity chamber at 100 % RH at room temperature 23 ± 2°C for 24 hours, then demoulded and cured in the humidity chamber for 7 days in the case $C_4A_3\bar{S}$ and $C_4A\bar{S}$, whereas cured up to 90 days for $\beta$-$C_2S$. At the end of any curing time, the hydration was stopped as described elsewhere [15, 16]. The combined water content of the dried sample was determined on the ignited weight basis after firing at 1000°C. The hydration products were studied by using XRD and DSC techniques.

## RESULTS AND DISCUSSION

### Hydration mechanism of calcium sulphoaluminate ($C_4A_3\bar{S}$)

#### *X-ray diffraction analysis*

The XRD patterns of hydrated sulphoaluminate phase as a function of curing time are illustrated in Figure 3. The hydration products formed were $C_4A_3\bar{S}.32H_2O$ (ettringite) and $C_4A\bar{S}.12H_2O$ (monosulphate). The type and the amount of hydrated products depend on the chemical constitutes of the clinker phases and the curing conditions. The XRD patterns indicate that calcium sulphoaluminate $C_4A_3\bar{S}$ hydrated up to 6 hours shows the presence of ettringite (AFt) and unhydrated calcium sulphoaluminate phase. The intensity of ettringite is highly increased while that of unhydrated $C_4A_3\bar{S}$ (yelimite) decreases and the appearance of monosulphate hydrate AFm with the curing time for 48 hours [17, 18]. This is mainly related to the fast hydration of sulphoaluminate $C_4A_3\bar{S}$ at early ages forming ettringite and amorphous $Al(OH)_3$ as well as monosulphate hydrate AFm [19]. The $AH_3$ and monosulphate hydrate AFm are certainly amorphous or microcrystalline as it was not observed in any XRD spectrum. As the curing time proceeds up

Table 1. Chemical oxide composition of the fired materials (wt. %).

| Materials | $SiO_2$ | $Al_2O_3$ | $Fe_2O_3$ | CaO | MgO | $SO_3$ | $Na_2O$ | L.O.I |
|---|---|---|---|---|---|---|---|---|
| $C_4A_3\bar{S}$ | 2.73 | 34.27 | 1.18 | 47.95 | 0.20 | 11.5 | 0.22 | 1.5 |
| $C_4A\bar{S}$ | 1.60 | 22.12 | 0.40 | 54.02 | 0.20 | 17.5 | 0.31 | 4.05 |
| $\beta$-$C_2S$ | 34.70 | 0.45 | 0.07 | 62.70 | 0.32 | – | 0.68 | 1.92 |

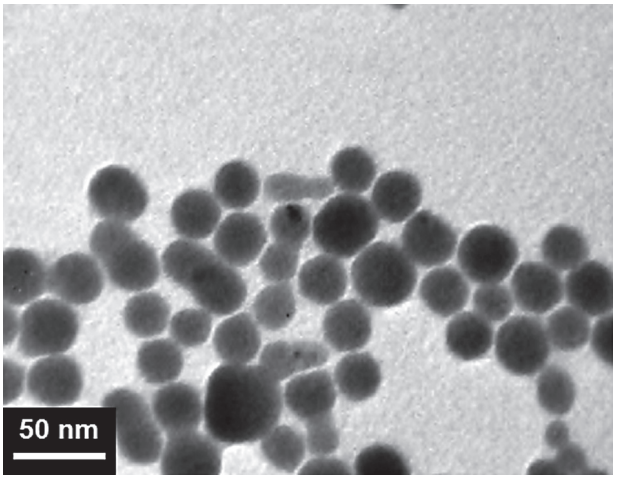


Figure 1. TEM micrograph of nano-$SiO_2$.

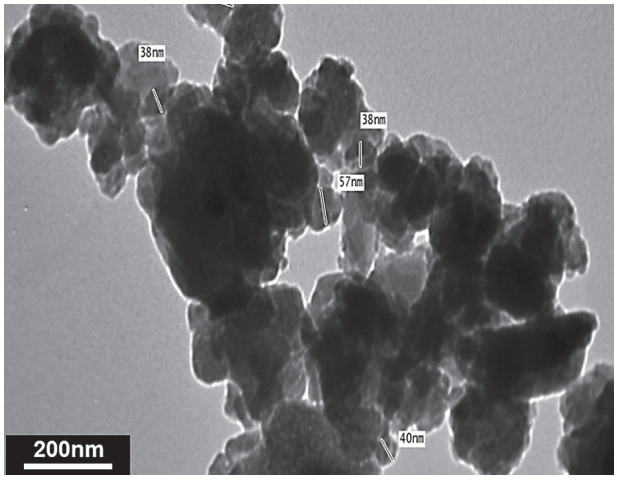


Figure 2. TEM micrograph of nano-aluminum hydroxide.

to 72 hours, the peak of ettringite increases strongly indicating that ettringite is the main hydration product of sulphoaluminte phase (8, 20).

The pattern shows the appearance of small peak of monosulphate hydrate at all curing times in a steady state. This may be due to the partial conversion of ettringite (AFt) to monosulphate hydrate (AFm) [19]. The transformation of ettringite to monosulphate hydrate may take place as follows [20]:

$$C_4A_3\bar{S} + 18H \rightarrow C_4A\bar{S}H_{12} + 2AH_3$$

$$C_4A\bar{S}_3H_{32} \rightarrow C_4A\bar{S}H_{12} + 2C\bar{S}H_2 + 16H$$

The hydration products depend on type of CSA cement used and on the amount of calcium sulphate added as well as the water to cement ratio [21]. The hydration mechanism in the presence of calcium sulphate is well characterized. If calcium is present, AFt is the first phase to form within the first hours in association with aluminum hydroxide [8], due to the reaction between $C_4A_3\bar{S}$ and calcium sulphate. The beginning of the AFt formation and of the yeelimite $C_4A_3\bar{S}$ hydration is related to the reactivity of the added calcium sulphate [22]. When the calcium sulphate depleted and/or in the absence of $Ca(OH)_2$, ettringite transformed into monosulphate hydrate ($C_4A\bar{S}H_{12}$, AFm) and with $AH_3$ [19].

### *Thermal analysis*

The DSC curves of hydrated calcium sulphoaluminate $C_4A_3\bar{S}$ as a function of curing time are shown in Figure 4. The figure shows the existence of endothermic peaks at 130, 180 and 270°C at all curing times of hydration. The endothermic peaks at 130 and 180°C are related to the dehydration of the lattice water of ettringite and the monosulphate hydrate respectively. These peaks increase with the curing time up to 3 days due to the continuous hydration of calcium sulphoaluminate phase [19, 23, 24]. The endothermic peak located at 270°C is mainly related to the dehydroxylation of $Al(OH)_3$. The peak of $Al(OH)_3$ increases from 6 hours and still constant up to 72 hours. The formation of monosulphate hydrate is due to the conversion of ettringite attributed to the lack of sulphate. It is clear that there is no thermal effect at 460°C indicating the absence of $Ca(OH)_2$. On prolong hydration, the endothermic peak of monosulphate hydrate increases with the presence of ettringite and $Al(OH)_3$ and/or $C_2AH_8$. The intensity of monosulphate has the same intensity from 24 up to 72 hours. In the presence of portlandite, monosulphate-hydroxy-AFm-solid solution can be formed [22]. When the CSA ($C_4A_3\bar{S}$) is hydrated in the absence of gypsum and lime the hydration is ettringite at early hours of hydration as follows:

$$3(C_4A_3\bar{S}) + 74\ H \rightarrow C_4A\bar{S}_3H_{32} + 3C_2AH_8 + 6AH_3$$

The hydration product after one day up to 48 hours is the formation of monosulphate hydrate with libration of $AH_3$

$$C_4A_3\bar{S} + 18H \rightarrow C_4A\bar{S}H_{12} + 2AH_3$$

The ettringite can be converted to monosulphate after its formation. Monosulphate hydrate AFm is certainly amorphous or microcrystalline as it is not observed in any XRD spectrum, but detected by DSC technique.

$$C_4A\bar{S}_3H_{32} \rightarrow C_4A\bar{S}H_{12} + 2C\bar{S}H_2 + 16H$$

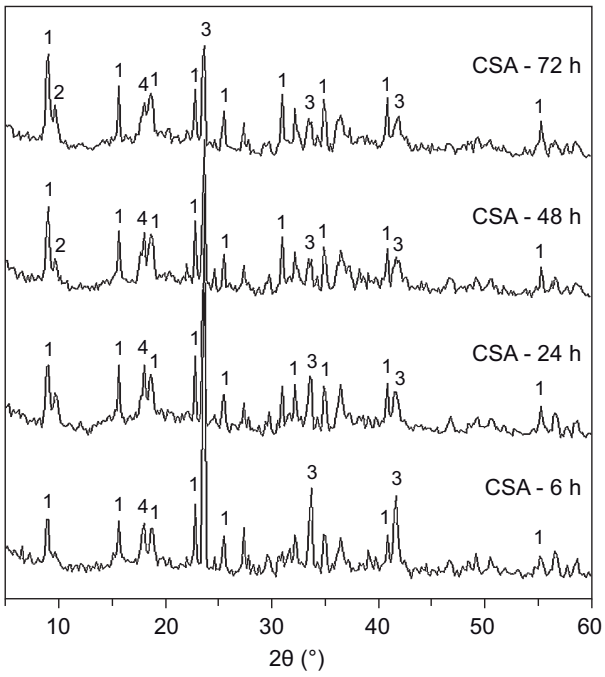


Figure 3. The XRD patterns of the hydrated calcium sulphoaluminate phase as a function of curing time (1 - AFt, 2 - AFm, 3 - $C_4A_3\bar{S}$, 4 - Mayenite).

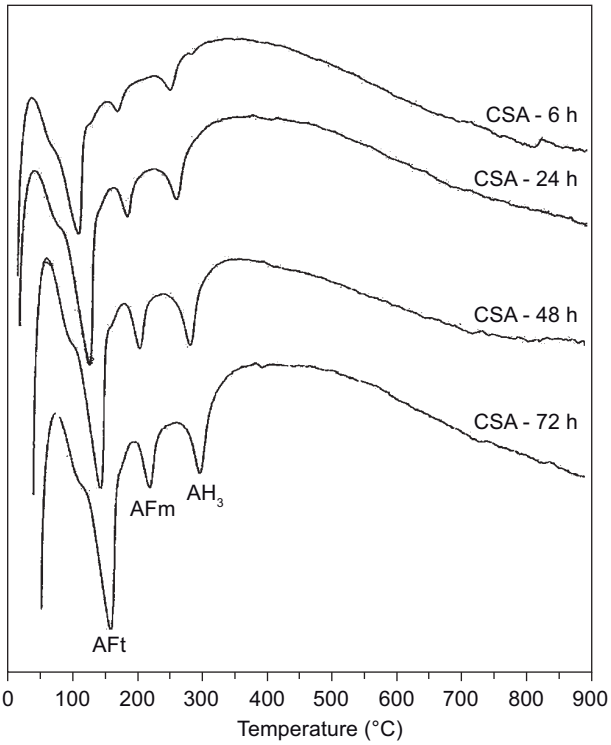


Figure 4. The DSC patterns of the hydrated calcium sulphoaluminate phase as a function of curing time.

Hydration characteristics of $C_4A\bar{S}$

*X-ray diffraction analysis*

The XRD patterns of the hydrated calcium aluminum monosulphate mix as a function of curing time are represented in Figure 5. XRD patterns of anhydrous aluminum monosulphate $C_4A\bar{S}$ hydrated for 6 hours shows the appearance of ettringite, very small peak of monosulphate hydrate and portlandite as well as unhydrated calcium sulphoaluminate $C_4A\bar{S}$. The results reveal also that the intensity of ettringite is highly increased with curing time up to 24 hours. This illustrates that anydrous calcium aluminum monosulphate is extensively hydrated forming ettringite and this is sustain with the consumption of unhydrated calcium aluminum monosulphate as well as and the reduction of portlandite after 24 hours. As the curing time proceeds up to 48 hours, the ettringite peak is decreased with the appearance of monosulphate hydrate peak. This is mainly attributed to the partial conversion of ettringite to monosulphate hydrate and amorphous $AH_3$ due to a lack of calcium sulphate [19]. When $Ca^{2+}$ and $SO_4^{2-}$ions are insufficient for the formation of ettringite in the hydration system, the decomposition of ettringite and the transformation to monosulphate hydrate occur [20]. The hydration of calcium aluminum monosulphate goes according to the following equation:

$$C_4A\bar{S} + 8C\bar{S}H_2 + 6CH + 10H \rightarrow 3C_4A\bar{S}_3H_{32}$$

It can be concluded that whatever the molar ratio of the anhydrous phase such as $C_4A_3\bar{S}$ or $C_4A\bar{S}$ the ettringite is the first hydrated phase formed in the early age of hydration [19].

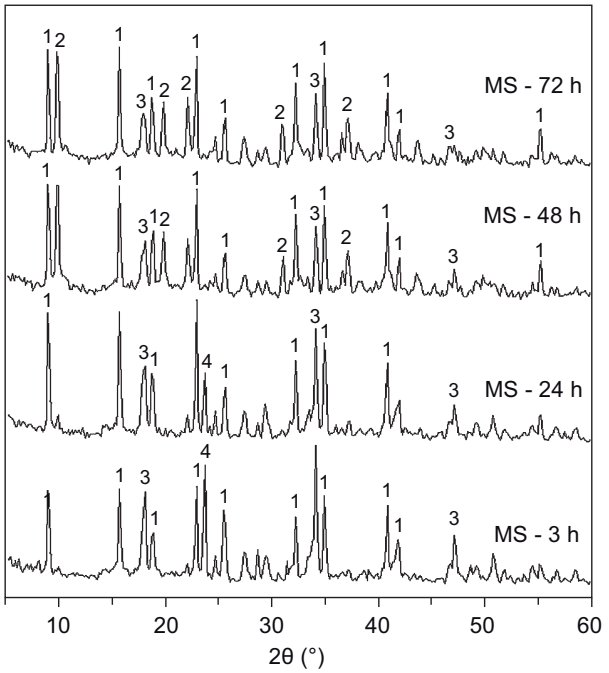


Figure 5. XRD patterns of the hydrated calcium aluminum monosulphate phase with curing time (1 - AFt, 2 - AFm, 3 - $Ca(OH)_2$, 4 - $C_4A\bar{S}$).

*Thermal Analysis*

DSC thermogrames of the hydrated mix of anhydrous monosulphate $C_4A\bar{S}$ illustrate four endotherms located at 170, 200, 250 and 450°C as well as weak endotherm at 700°C as shown in Figure 6). The first peak is mainly due to ettringite, whereas the second endothermic at 200°C is related to the monosulphate hydrate [19]. The third and fourth peaks are due to the dehydroxylation of $C_4AH_{13}$ and/or $C_2AH_8$ as well as portlandite $Ca(OH)_2$ .The appearance of $C_4AH_{13}$ and/or $C_2AH_8$ is mainly due to the deficiency of anhydrite $CaSO_4$ to give ettringite. Therefore, the detection of ettringite with monosulphate hydrate leads to the presence of hydrated aluminate phases such as $C_2AH_8$ and/or $C_4AH_{13}$. On other side, the endotherm at 700°C is due to the calcination of $CaCO_3$. The ettringite and portlandite formed after 6 hours up to 24 hours. After 48 hours the monosulphate hydrate is appeared from the conversion of some ettringite with the release of $Al(OH)_3$ [19]. The $C_4AH_{13}$ and/or $C_2AH_8$ are appeared at 48 hours. After 7 days some hydrated phases are present. The transformation of ettringite to monosulphate is ascribed to the lack of gypsum [19]. In a previous work [25] the mole ratio of monosulphate was prepared from $CaCO_3$, alumina and gypsum then fired at 1350°C and hydrated up to 7 days. DTA of the hydrated mix illustrates the formation of ettringite and monosulphate hydrate with residual $Ca(OH)_2$ after 6 hours. The endotherm of monosulphate hydrate decreases with the increase of ettringite. After 7 days of hydration, the main hydration product is ettringite with the increase of portlandite. These results are not in

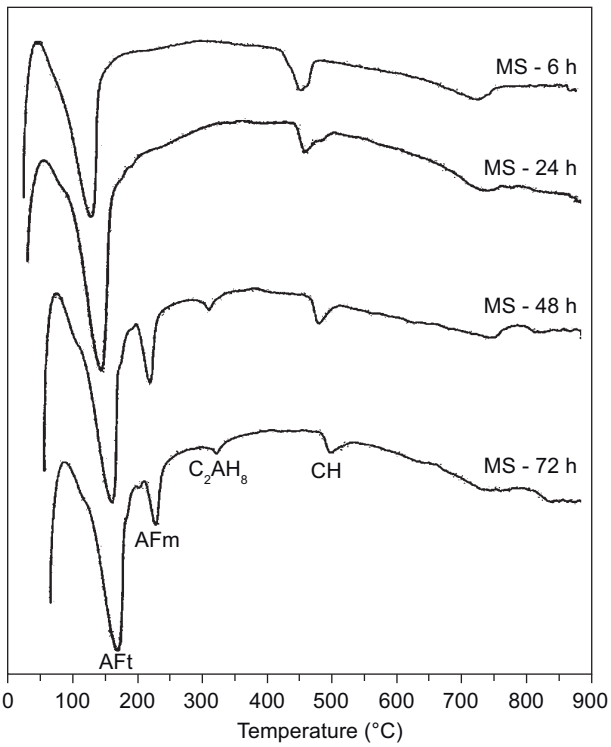


Figure 6. The DSC patterns of the hydrated calcium aluminum monosulphate phase as a function of curing time.

agreement with those of our present investigation. This may be due to the low reactivity of monosulphate because this mix was prepared from traditional materials whereas the present mix was prepared from nano-materials, with highly reactive nano-$C_4A\bar{S}$.

## Hydration characteristics of reactive belite ($C_2S$) phase

### *X-ray diffraction analysis*

The XRD patterns of the hydrated belite phase as a function of curing time are seen in Figure 7. The Figure illustrates the presence of belite and calcium silicate hydrate as well as portlandite. The results indicate that the intensity of $C_2S$ is slightly decreased with the curing time up to 7 days. On the contrary, the intensity of calcium hydroxide and calcium silicate hydrate peaks are slightly increased. This is due to the slow rate of hydration of belite at early ages [26]. As the hydration proceeds, the intensity of $C_2S$ is highly decreased at 28 days of curing time indicating the low rate of hydration of belite.

### *Thermal analysis*

The DSC curves of hydrated belite phase as a function of curing time are represented in Figure 8. The DSC curves illustrate the presence of endothermic peaks at about ~100 and 465°C as well as 730°C. The endothermic effect at 100°C is caused by the dehydration of the bound water from amorphous calcium silicate hydrate phase (CSH). Meanwhile, the endothermic peak at 450°C is related to the dehydroxylation of $Ca(OH)_2$. The area under characteristic peak of CSH increases with the curing time attributed to the continuous hydration of $C_2S$ forming CSH and $Ca(OH)_2$ [27].

It is clear that there are different forms of CSH up to 7 days whereas at 28 days CSH is detected at ~100°C. This is due to the decrease of other forms of CSH which can be easily decomposed at lower temperature. The endothermic at ~700°C is due to the decomposition $CaCO_3$ which increases with curing time on the expense of $Ca(OH)_2$ [28].

## Chemically combined water contents

### *Sulphoaluminate phase*

The chemically combined water contents of (CSA and MS) as a function of curing time are graphically plotted in Figure 9. The results indicate that the chemically combined water contents increase gradually with curing time for hydrated CSA and MS mixes. The Figure shows that the chemically combined water content for hydrated CSA ($C_4A_3\bar{S}$) phase increases sharply at the early hours up to 48 hours and increases with lower content up to three days [23]. This is mainly attributed to the rapid formation of ettringite which has a high content of water. This indicates that there is small variation in the hydration products after 72 hours. As curing time increases up to 24 hours chemically combined water content of CSA is sharply enhanced. At latter ages the rate of increase of chemically combined water content is diminished up to 72 hours.

Sample hydrated of MS for 48 hours gives higher chemically combined water content than that at 24 hours. This is related to the formation of higher amount of

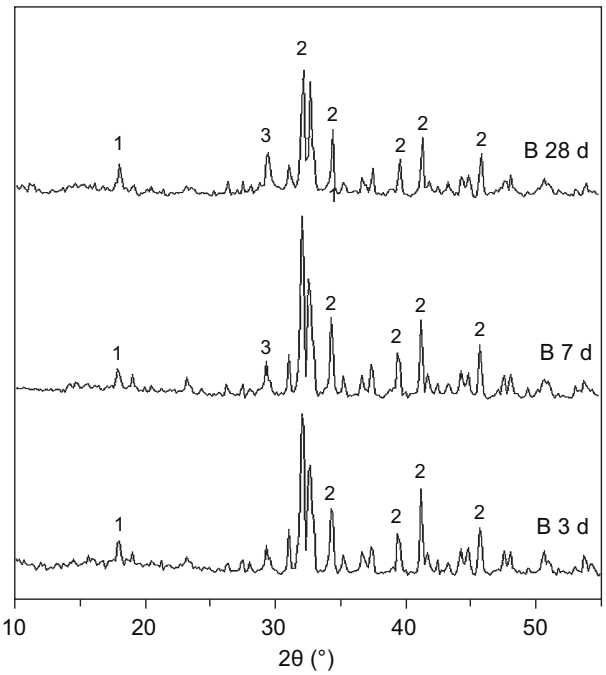


Figure 7. XRD patterns of the hydrated belite phase as a function of curing time (1 - $Ca(OH)_2$, 2 - $C_2S$, 3 - CSH).

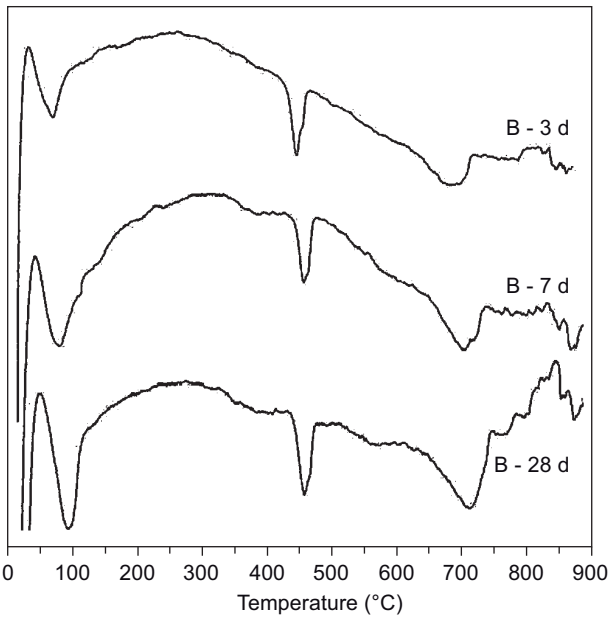


Figure 8. DSC patterns of the hydrated belite phase as a function of curing time.

ettringite in addition to monosulphate which have higher combined (lattice) water. On the other side, the chemically combined water content of sample hydrated for 72 hours shows lower rate of combined water than that from 24 up 48 hours. This is mainly due to that there is small difference in the hydration products from 48 hours to72 hours.

The chemically combined water content of MS pastes is higher than that of CSA after 6 hours of hydration. This is mainly attributed to the formation of ettringite in addition to portlandite, therefore, the chemically combined water content increases. The monosulphate mix gives higher chemically combined water content than those of CSA phase. This is due to that the hydration of MS gives ettringite, monosulphate in addition to portlandite theses phases give higher water content.

*Traditional and active belite phases*

Figure 10 illustrates the chemically combined water contents of traditional β-dicalcium silicate prepared from $CaCO_3$ and gypsum. Chemically combined water contents shows a very little increase up to 28 days, this is attributed to the low reactivity of traditional β-dicalcium silicate at early ages. The low hydration of this phase is due to its microstructure form [5, 6]. This has been attributed to the higher thermodynamic stable structure of traditional β-dicalcium silicate.

The active belite phase with 27 nm crystal size gives higher chemically combined water contents in comparison with that of traditional β-dicalcium silicate. Singh [26] studied the hydrothermal synthesis of β-$C_2S$ from rice husk and fly ashes. Results have shown that hydrothermally prepared β-$C_2S$ is also, highly reactive. The high reactivity of belite may be due to nano-crystal size and higher surface area. Active belite phase hydrated to form nano-size CSH which might have a porous structure and does not hinder the approach of water molecules to the fresh belite. In this work of the active belite was synthesized from nano-$Ca(NO_3)_2$ and nano-silica which has the crystal size of 27 nm.

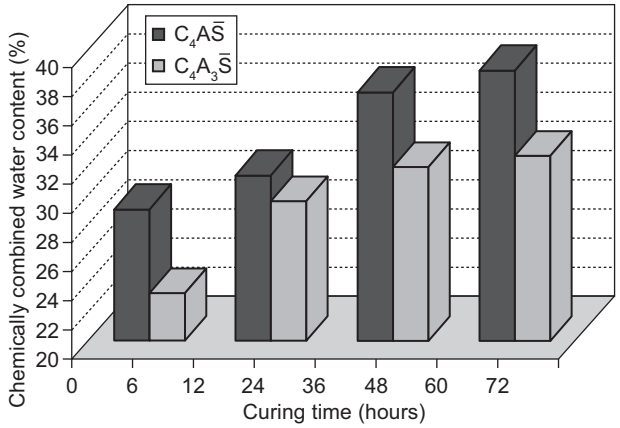


Figure 9. Chemically combined water contents C4A3S̄ and C4AS̄.

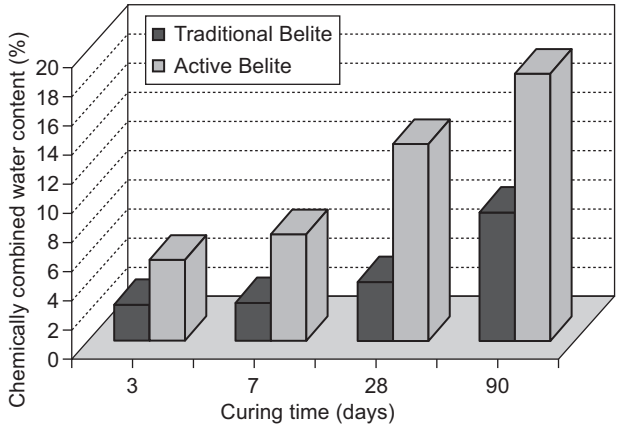


Figure 10. Chemically combined water contents of traditional and active belite as a function of curing time.

## CONCLUSION

From the above findings it can concluded that:

1. The rate of hydration of active belite is higher than that of traditional belite phase as shown from the higher chemically combined water contents up to 90 days of hydration.
2. The hydration of $C_4A_3\bar{S}$ gives ettringite at early ages of hydration in spite of low content of $CaSO_4$ which converts to monosulphate, monosulphate hydrate AFm is certainly amorphous or microcrystalline as it is not observed in any XRD spectrum. The monosulphate is very small in comparison with ettringite. The sulphoaluminate phase remains free up to 72 hours and cannot be completely hydrated.
3. The hydration of monosulphate mix shows ettringite as the main hydrated sulphoaluminate up to 24 days. As the hydration proceeds the monosulphate hydrate appeared at 48 hours and still constant at 72 hours in addition to appreciable amount of ettringite.

Acknowledgment

*The authors would like to thank Prof. Dr. Mohamed Heikal, Professor of Inorganic Chemistry and Building materials, Chemistry Department, Faculty of Science, Benha University, Benha, Egypt, for his great help throughout the interpretation of the results of this article.*

References

1. Hui Li., Hui-gang Xiao, Jie Yuan, Jinping Ou.: Compos, part B *35*, 185 (2004).
2. Hanehara S., Lchikawa M.: Journal of the Taiheiyo Cement Corporation, *141*, 47 (2001).

3. Gengying Li.: Cem. Concr. Res. *34*, 1043 (2004).
4. Ginebra MP., Driessens FC., Planell JA.: Biomaterials, *25*, 3453 (2004).
5. Sharara A.M., El-didamony H., Ebied E., Abd-El-Aleem S.: Cem. Concr. Res. *24*, 966 (1994).
6. Kasselouri V., Tsakiridis P., Malami C.H., Georgali B., Alexandridou C.A.: Cem. Concr. Res. *25*, 1726 (1995).
7. Kurdowski W., Duszak S., Trybalska B.: Cem. Concr. Res. *27*, 51 (1997).
8. Glasser F.P., Zhang L.: Cem. Concr. Res. *31*, 1881 (2001).
9. Abd El-Raoof F.: (2008): Ph.D. Thesis, Faculty of Science, Zagazig University, Egypt (2008).
10. Mathew L., Narayankutty SK. in: International conference on advance in polymer technology, p. 279, India (2010).
11. Tupin G.S.: *Practical Inorganic Chemistry*, (Classic Reprint), 2010.
12. El-Didamony H., Khalil Kh.A., Ahmed I.A., Heikal M.: Constr. Build. Mater. *35*, 77 (2012).
13. El-Didamony H., Sharara AM., Helmy I. M., Abdel-Aleem S.: Cem. Concr. Res. *26*, 1179 (1996).
14. ASTM Designation C191: *Standard test method for normal consistency and setting time of Hydraulic Cement* ", Annual book of ASTM standard ,04.01, 2008.
15. El- Didamony H., Haggag M.Y., Abo-El-Enein S.A.: Cem. Concr. Res. *8*, 351 (1978).
16. El-Didamony H.: Thermochimca Acta *35*, 201 (1980).
17. Drábik M., Kaprálik I., Oliew G., Wieker W.: J. Thermal Analysis *33*, 679 (1988).
18. El-Didamony H., Khalil Kh.A., Heikal M., Ahmed I.A.: J. Thermal Analysis and Calorimetry, submitted, 2012.
19. LiaoY., Xiaosheng W., Guowei Li.: Construct Build. Mater. *25*, 1572 (2011).
20. Pelletier L., Winnefeld F., Lothenbach B.: Cem. Concr. Comp. *32*, 497 (2010).
21. Winnefeld F., Lothenbach B.: Cem. Concr. Res. *40*, 1239 (2010).
22. Winnefeld F., Barlag S.: ZKG Int. 12, 42 (2009).
23. Bernardo G., Telesca A., Valenti V.G.: Cem. Concr. Res. *36*, 1042 (2006).
24. Gastaldi D., Canonico F., Boccaleri E.: J. Mater. Sci. *44*, 5788 (2009).
25. Henning O., El-Didamony H., Hanna K.M.: Wiss. Zeit. Hochshul. Archit. Bauwesen *19*, 465 (1972).
26. Singh N.B.: Progress in Crystal Growth and Characterization of Materials *52*, 77 (2006).
27. Ramachandran V.S., Paroli R.M., Beaudoin J.J., Delgado A.H.: *Hand book of thermal analysis of construction materials* , Noyes Publ., New York, 2002.
28. El-Didamony H., Ali H.A., Mostafa K.A.: Indian J. Eng. Mater. Sci. *3*, 248 (1996).